1. SCIENTIFIC RESEARCH

NEUTRON NUCLEAR PHYSICS

In 2014, in FLNP the scientific activity in the field of neutron nuclear physics was carried out in the following traditional directions: investigations of time and space parity violation processes in neutron-nuclear interactions; studies of the fission process; experimental and theoretical investigations of fundamental properties of the neutron; gamma-spectroscopy of neutron-nuclear interactions; atomic nuclear structure, obtaining of new data for reactor applications and for nuclear astrophysics; experiments with ultracold neutrons. The greater part of the fundamental investigations was conducted on the modernized IBR-2 reactor, IREN pulsed resonance neutron source and EG-5 electrostatic generator. Of particular note is the wide range of applied research using NAA. A number of investigations in the field of fundamental physics and ultracold neutron physics were performed on the neutron beams of nuclear research centers in Germany, China, USA, France, Switzerland.

Modernization of the IREN facility

In 2014, the modernization of the IREN facility was continued (**Fig. 27**). Its purpose is the achievement of design parameters of the neutron source (intensity of the order of 10^{13} n/s) by 2016. The project involves the assembling of the second accelerating section, installation of new modulators and replacement of klystrons. By now, two new modulators producing high-voltage pulses with 180 MW pulse power at a repetition rate of up to 120 Hz and two E3730A Toshiba 50MW klystrons have been purchased. The implementation of the project will allow working with a repetition rate of 50 Hz at an electron energy of ~170 MeV, thus providing an average beam power of ~1.5 kW. An additional increase in the neutron yield can be achieved by replacing the tungsten neutron production target with a U-238 target. The installation of the second accelerating section, new RF-power sources and a uranium target calls for a thorough modernization of the engineering infrastructure of the IREN facility, which is currently underway. In 2014 an air-conditioning and ventilation system was installed in the accelerator halls; also, work began on upgrading the power supply system of building 43. Along with these activities in 2014 the IREN facility operated for 1,360 hours for physics experiments.

Fig. 27. Lifting of modulators to the accelerator hall through a specially made opening.

I. Experimental and methodological investigations

Modernization of multi-detector system "Romashka-INRNE"

The multidetector system "Romashka-INRNE" consists of 12 NaI(Tl) detector modules and is designed for measuring neutron cross sections at the IREN facility. The detector system was assembled and installed on IREN beamline №4. Twelve emitter repeaters of signals from photomultipliers of γ-ray NaI(Tl) detectors were manufactured, tested and installed. A series of measurements was performed using standard spectrometric gamma sources SSGS (Cs-137 and Co-60) for different source-detector geometries for experimental and model (analytical) determination of gamma-radiation detection efficiency of non-point sources. The experimental values of the efficiencies were obtained; the determination of the model ones is in progress. Using the computer program FLUKA the (neutron, gamma)-field intensity distribution was calculated in the area of the gamma-spectrometer "Romashka-INRNE" on IREN beamline №4 (**Fig. 28**)

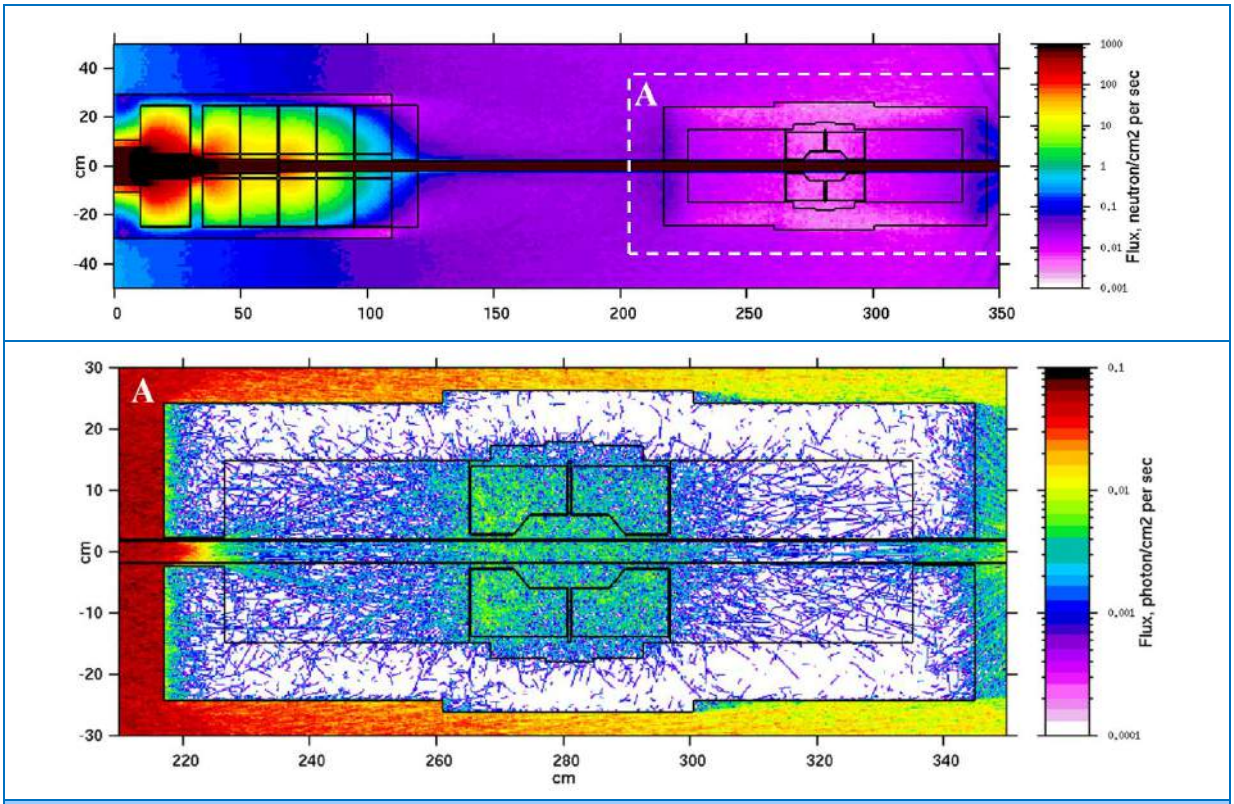

Fig. 28. Intensity of the neutron field in the area of a shielding collimator (SC) of the 12-detector gamma spectrometer "Romashka-INRNE" (top) and of γ-rays in it when a beam of neutrons and γ-rays from the IREN facility falls on the SC input.

Project TANGRA: Development and optimization of the tagged neutron method for elemental analysis and nuclear reaction studies

The multidetector system "Romashka" consisting of 24 hexagonal NaI(Tl) crystals was tested using γ-rays from inelastic scattering of 14-MeV neutrons by carbon, $^{12}C(n,n'\gamma)^{12}C$. A neutron generator ING-27 was used as a source of tagged neutrons. Neutrons are produced in the reaction d + 3H → 4He(3.5MeV) + n(14.1MeV) in which α-particles and neutrons fly apart in almost opposite directions, and therefore, with a knowledge of α-particle momentum direction, the neutron momentum direction can be determined with high accuracy. Thus, neutrons can be tagged using a multichannel

α-detector built into a portable neutron generator, which accelerates deuterons up to energies of 80-100 keV and focuses them on a tritium target. A 64-pixel silicon detector built into ING-27 was used to detect α-particles. The measurement of the time interval between the signals from α- and γ-detectors allows one to determine the distance from the point of neutron emission in the d-t reaction to the point of interaction between the tagged neutron and the nucleus of the substance under study (velocity of 14.1-MeV neutron is 5 cm/ns). Thus, it is possible to determine all three coordinates of the point where characteristic γ-radiation is generated. In the experiment, time and amplitude spectra were measured in coincidence with the signals from the central silicon pixel which corresponds to the neutron cone directed at a graphite target positioned in the center of the detector system "Romashka" (**Fig. 29**).

Fig. 29. Experiment to study inelastic scattering of 14-MeV tagged neutrons by ^{12}C nuclei: 1 - tagged neutron generator ING-27, 2 - polyethylene, 3 - lead, 4 – gamma-detection system "Romashka", 5 - graphite cube.

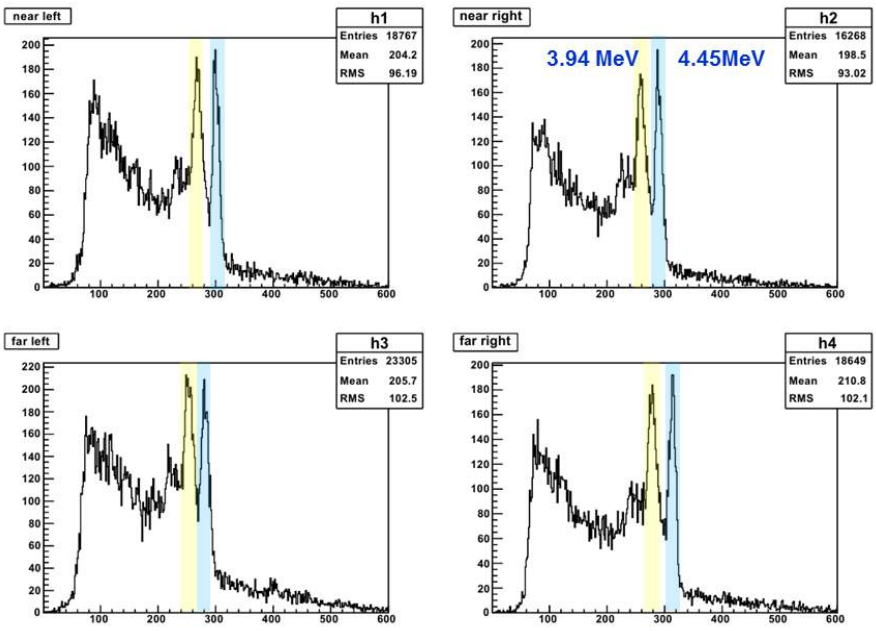

Fig. 30. Amplitude spectra of γ-rays from 4 sections of the "Romashka" setup.

The detectors were shielded from exposure to the direct neutron beam from the generator using a combined collimator made of polyethylene and lead. The experiment has shown that the obtained time and amplitude resolution is sufficient for conducting measurements with the tagged neutron method using the combination of ING-27 + "Romashka". The amplitude spectra of γ-rays from 4 NaI(Tl) sections are presented in **Fig. 30.**

The experimental studies and simulation of the most effective shielding were carried out to reduce the direct neutron flux coming from the generator to gamma- or neutron detectors. An experimental stand was constructed which allows measuring the efficiency of detector shielding using different shielding materials with thicknesses varying from 0 to 50 cm. NaI(Tl), BGO, stilbene crystal and BC-501 liquid scintillators were used as detectors. The last two scintillators allow neutron/gamma pulse shape discrimination. Different combinations of lead, iron and borated polyethylene were tested as shielding materials. The most suitable compositions of the combined shield for the projected experiments were experimentally found to be: 30 cm (Fe) + 10 cm (BPE) + 10 cm (Pb) and 20 cm (Fe) + 10 cm (BPE) + 20 cm (Pb). More detailed results will be published in the journal *Physics of Elementary Particles and Atomic Nuclei, Letters* (in Russian) and an abridged version of the paper will be submitted to *Nucl. Instr. and Methods* (in English). **Figure 31** presents the layout of the experiment and one of the graphs showing the degree of attenuation of 14-MeV neutrons from the generator ING-27 by the combined shield consisting of Fe and Pb layers of different thicknesses.

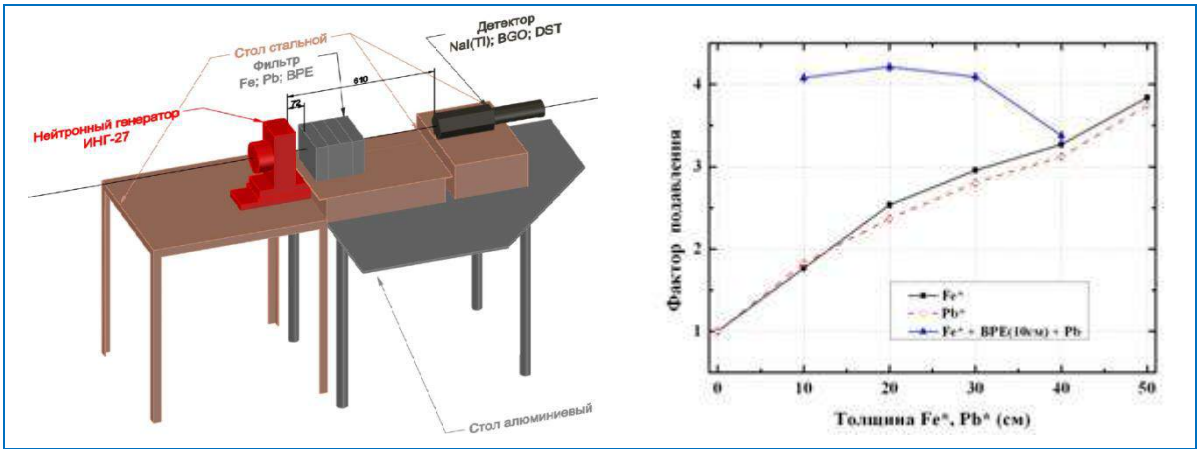

Fig. 31 Left: Layout of the experiment to optimize shielding against 14-MeV neutrons. Right: neutron (and γ-ray) attenuation factor measured with a hexagonal NaI(Tl) detector as a function of the thickness of Fe and Pb layers.

A setup was designed and constructed for measuring the angular distribution of γ-quanta emitted in the inelastic scattering of 14-MeV neutrons by carbon (**Fig. 32**). NaI(Tl) γ-detectors are arranged in the horizontal plane at different angles with respect to the direction of the neutron beam hitting the target. A collimator, which provides maximum shielding of detectors from exposure to the direct neutron beam from the generator was manufactured. The collimator dimensions are minimized to reduce the background from fast neutrons scattered by it. The experiments are planned to be conducted at the end of 2014 - the beginning of 2015.

1. SCIENTIFIC RESEARCH

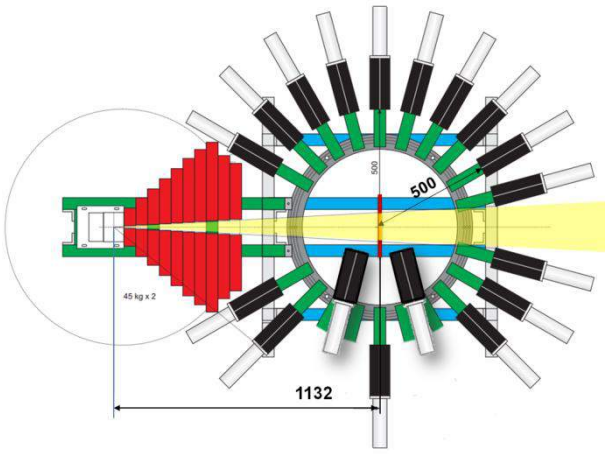

Fig. 32. Layout of the setup for measuring the angular distribution of γ-quanta emitted in the inelastic scattering of 14-MeV neutrons: tagged neutron generator ING-27; combined shield; set of neutron and γ-ray detectors.

Activities on the preparation of the (n,e) scattering experiment

In 2014, the debugging of programs for the 8-channel time encoder and PC-based measuring module of the AURA setup was continued. At the IREN neutron facility the hours-long testing of the operation of the setup (including the control of the turntable and collection of spectra) was carried out [3]. In the course of further testing of the AURA setup four week-long measurement cycles were conducted to measure the anisotropy of slow neutrons with energies in the range of 0.005-10 eV scattered by metallic vanadium, which is used as a calibration sample in condensed matter physics experiments. Each measurement cycle consisted of a series of hour-long exposures with recording of spectra measured by the detectors upon completion of each of them. Since there are four detectors on the turntable and each of them alternately measures the neutron scattering in forward and backward directions (positions of the detectors with respect to the neutron beam change with the turntable rotating through 180° upon completion of each exposure), the anisotropy is calculated as the geometric mean of the ratio of forward/backward counts from all the detectors:

$$R = \sqrt[4]{\frac{(N_s - N_{bg})_{2f}(N_s - N_{bg})_{3f}(N_s - N_{bg})_{1f}(N_s - N_{bg})_{4f}}{(N_s - N_{bg})_{1b}(N_s - N_{bg})_{4b}(N_s - N_{bg})_{2b}(N_s - N_{bg})_{3b}}},$$

where under the radical sign the numerator is the total counts with the subtraction of the background recorded by the detectors in the neutron forward scattering position, and the denominator is the sum of detector counts in the backscattering position. The relative error of the ratio was calculated as

$$\delta R = \sqrt{\sum_1^8 \delta^2 (N_s - N_{bg})}, \text{ where } \delta(N_s - N_{bg}) = \frac{\sqrt{(N_s + c^2 N_{bg})}}{N_s - cN_{bg}} \text{ and } c = \frac{M_s}{M_{bg}}.$$

M_s and M_{bg} – monitor counts with and without a sample, respectively. The results are presented in **Fig. 33**.

The data of [4] are in good agreement with the R(E) relations obtained earlier in the experiments at the IBR-2 reactor and suggest that at neutron energies below 0.1 eV the scattering by vanadium has an anisotropic behavior different from purely kinematic anisotropy of neutron scattering by a free nucleus.

The Monte Carlo calculations are being continued to refine the kinematic correction for the asymmetry of thermal neutron scattering by krypton, which is required for the experiment on the

extraction of a precise n,e-scattering length value from the angular anisotropy of slow neutrons scattered by an inert gas at atmospheric pressure.

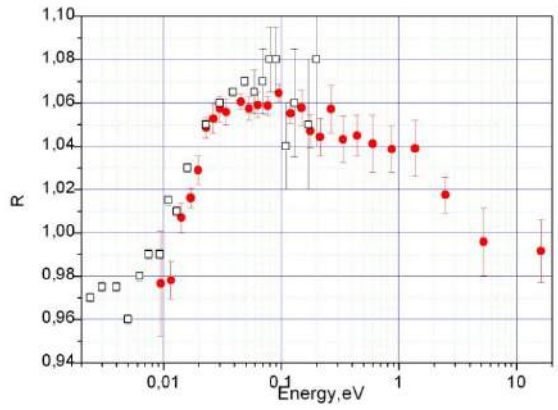

Fig. 33. Averaged R(E) relations from [3] (points) and data obtained in 2004 on IBR-2 beamline 11b (open squares).

Measurement of parameters of polarized neutron beam at the KOLKHIDA setup

In 2014, on IBR-2 beamline №1 on the polarized neutron spectrometer after repeated refitting of in-channel collimators the work was carried out to determine parameters of the polarized neutron beam. The parameters were determined in the neutron energy range of 0.062-2.3 eV using the two-converter method. A polarized neutron beam with polarization P_n = 0.98 was obtained. The layout of the polarized neutron setup is shown in **Fig. 34**. The primary-neutron spectrum is formed in the moderator of the reactor. The neutrons emerging from the moderator go through the channel in the biological shield and pass through primary collimator 1. Prior to entering the analyzer, the neutrons go through Soller collimator *2*. In order to polarize neutrons and to analyze their polarization, we use Co-Fe single crystals.

The intensity and energy spectrum of the primary neutron beam incident on the polarizer were measured using the RM-70 fission chamber. The chamber was placed at a flight distance of 13.5 m. As a result, we obtained data on the neutron intensity and spectrum in an energy range of 10-200 meV (**Fig. 35**). The neutron flux in the specified energy range was $1.0 \cdot 10^6$ n/cm^{2}s.

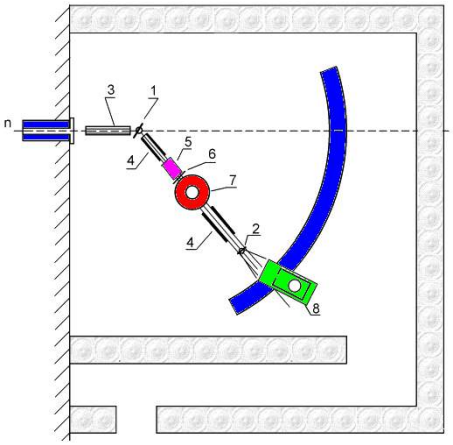

Fig. 34. 1 – primary collimator; 2 – Soller collimator; 3 – polarizer crystal; 4 – guiding field electromagnets; 5 – Mezei flipper; 6 – shim; 7 – cryostat; 8 – analyzer crystal; 9 – detector.

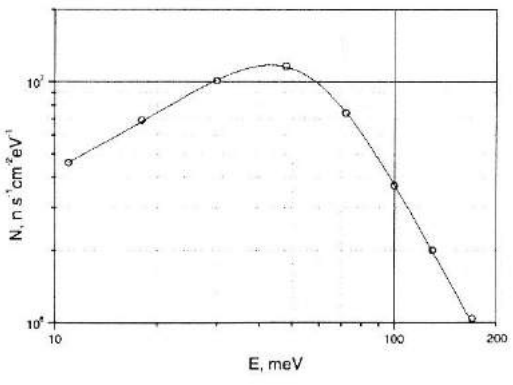

Fig. 35. Dependence of the neutron flux density on the energy of neutrons incident on the polarizer.

1. SCIENTIFIC RESEARCH

For the Co-Fe single crystal, the neutron diffraction was measured in the Laue geometry for different angles θ in a range of 3°-19° at which the incident neutrons hit the (200) surface (**Fig. 36, 37**). The measured values of the neutron wavelengths and energies for the listed angles θ are presented in Table 1. The reflected beam maximum was determined by varying the θ angle. The detector counting rate n_1 and the intensity I_1, which takes into account the detector efficiency and the reflected beam area (s $\cong$ 4 cm^2), are given in **Table 1**.

Table 1. Parameters of the polarized neutron beam**.**

Angle θ (deg)	19	12	6	4	3
Wavelength λ (Å)	1,15	0,74	0,37	0,25	0,19
Energy En (eV)	0,062	0,15	0,6	1,3	2,3
Detector counting rate	800	270	65	33	22
after the polarizer n_1 (s^{-1})	430	200	80	60	50
Polarized beam intensity I_1, n/cm^2s	70	23	3,1	0,6	0,2
Detector counting rate after the analyzer n_2, s^{-1}	70	23	3.1	0.6	0.2

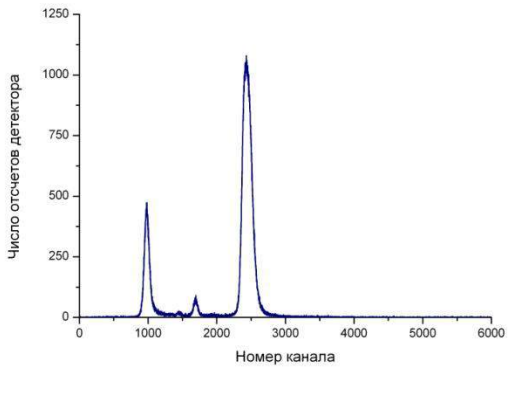

Fig. 36. Time-of-flight neutron spectra after the polarizer obtained for 3 min. θ = 19°.

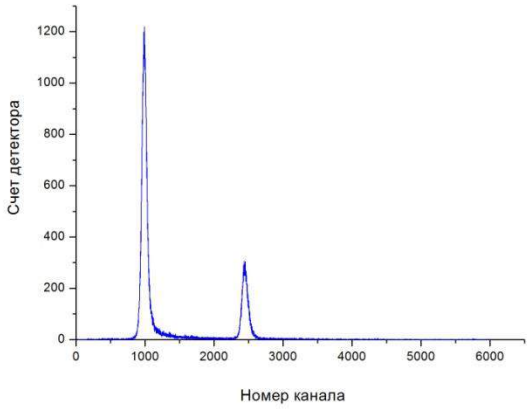

Fig. 37. Time-of-flight neutron spectra after the analyzer obtained for 10 min. θ = 19°.

Observation of transition from Laue diffraction to Bragg diffraction

In the framework of preparation of experiments to investigate the weak neutron-nucleus interaction in neutron diffraction, experimental studies of neutron diffraction by a potassium bromide single crystal were carried out on IBR-2 beamline 1. A potassium bromide single crystal was chosen due to a rather large P-odd effect in the transmission found in the p-wave resonance of bromine-81. In particular, an interesting phenomenon—transition from Laue diffraction to Bragg diffraction—was revealed.

The incident neutron beam had a cross section of 4x40 mm and divergence $4x10^{-3}$ rad. A plate of cadmium or borated polyethylene was placed in front of the single crystal to shield its side surface from the neutron beam. The similar plate was placed behind the single crystal and covered either its side surface in the Laue neutron diffraction geometry or the end surface when observing the transition

from Laue diffraction to Bragg diffraction. **Figure 38** presents the TOF spectra obtained in two geometries. The simplest explanation for the observed effect is the crystal twinning. To test this hypothesis, the single crystal was rotated through 180 degrees around the scattering vector. **Figure 39** shows the TOF spectra of these measurements.

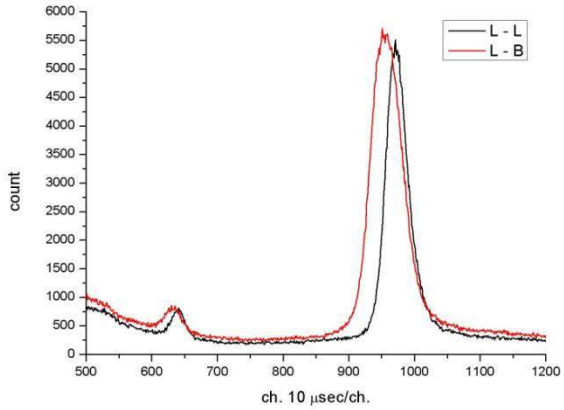

Fig. 38. Black line corresponds to neutron diffraction in the Laue geometry, the red line – transition from Laue diffraction to Bragg diffraction.

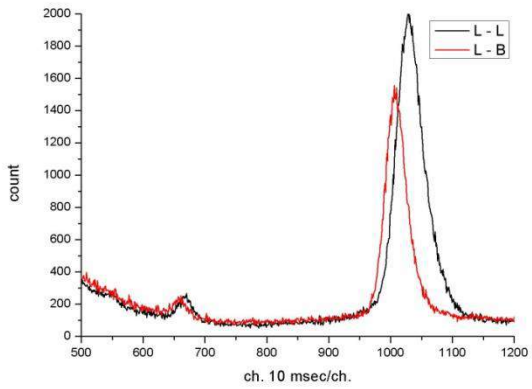

Fig. 39. Single crystal is rotated through 180° around the scattering vector. The black line corresponds to neutron diffraction in the Laue geometry, the red line – transition from Laue diffraction to Bragg diffraction.

One can see that the spectrum character is unchanged. In principle, such an effect can be observed in a deformed single crystal or due to the weak neutron-nucleus interaction. If the single crystal is deformed, by rotating it through 180 degrees around the axis perpendicular to the scattering vector one should expect the opposite peak distribution. The results of these measurements presented in **Fig. 40** support the hypothesis about a deformed single crystal. The same effect is observed in three potassium bromide single crystals produced at different times.

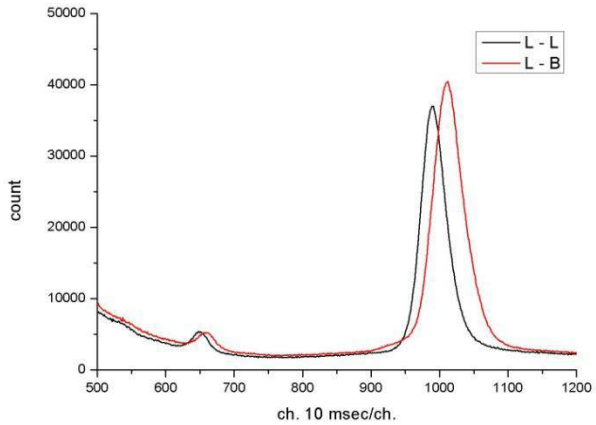

Fig. 40. Single crystal is rotated through 180° around the axis perpendicular to the scattering vector. The black line corresponds to neutron diffraction in the Laue geometry, the red line – transition from Laue diffraction to Bragg diffraction.

Development of techniques for fission physics investigations

Detection of ternary and quaternary spontaneous fission of ^{252}Cf using ΔE-E telescopes based on silicon pixel detector TimePix

In 2014, in cooperation with TU Prague the measurements of ternary and quaternary spontaneous fission of ^{252}Cf were carried out using Timepix detectors. To identify ternary particles, the ΔE-E method was used to separate light charged particles by charge. A thin (12 μm) silicon detector

1. SCIENTIFIC RESEARCH

was used as a ΔE-detector and a TimePix pixel detector with a 300 μm-thick sensor layer – as an E-detector.

The layout of the experimental setup is shown in **Fig. 41**. A spontaneous fission source ^{252}Cf and two assemblies of ΔE-E detectors were placed in a vacuum chamber. Aluminum 31 μm-thick foil was placed between the source and the detector. The foil provided the full absorption of fission fragments and alpha particles from spontaneous alpha decay of Californium (6.2 MeV). Thus, the detectors recorded only long-range light charged particles from ternary fission.

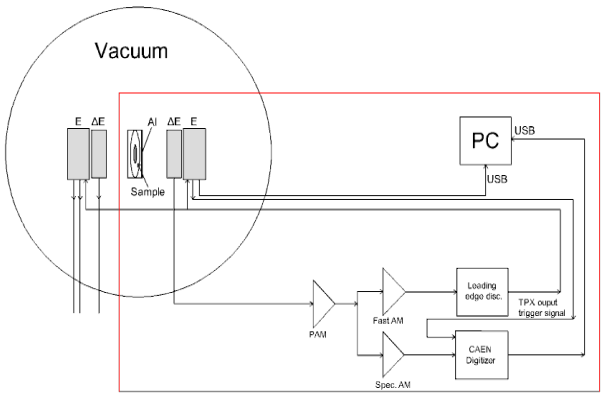

Fig. 41. Layout of the experimental setup.

Figure 42a shows the two-dimensional ΔE-E separation curves of light charged particles. In the experiment we managed to detect particles ranging from hydrogen to beryllium. One can clearly see the most intensive region of alpha particles. The energy spectra were plotted for each type of particles. The preliminary corrections for energy losses in the aluminum foil and ΔE detector were calculated using the Srim program. **Figure 42b** demonstrates the measured energy distribution of alpha particles in the ternary fission of ^{252}Cf in comparison with the published data.

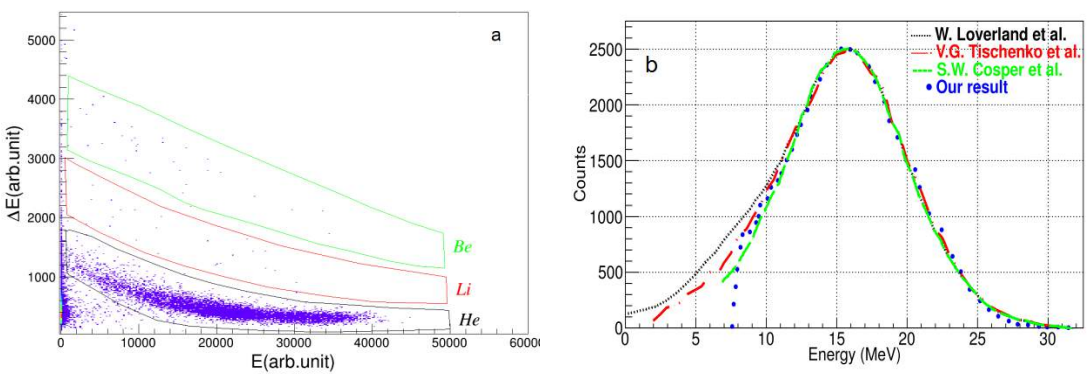

Fig. 42. (a) ΔE-E spectrum of light charged particles. (b) The energy spectrum of alpha particles.

Figure 43 (a, b, c) presents the energy spectra of helium, lithium and beryllium. Each spectrum was fitted with the Gaussian curve and the light charged particle yields were determined. The experiment was also aimed at searching for even more rare fission mode than ternary fission – quaternary fission, when in addition to two main fragments two light charged particles are emitted. The probability of this process is extremely low and reaches 10^{-6}-10^{-7} of the normal binary fission. As a rule, two alpha particles are formed in quaternary fission, and can be emitted either independently

(true quaternary fission), or as a result of decay of an unstable nucleus of ^{8}Be emitted as a third particle (pseudo-quaternary fission).

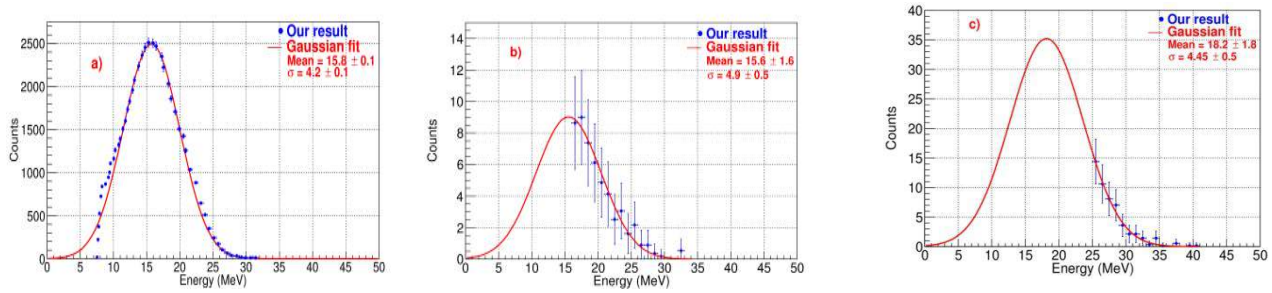

Fig. 43. The energy spectra of light charged particles: (a) He, (b) Li, (c) Be.

Seventy two events were observed, in which two particles were detected simultaneously in one or two telescopes. A symmetrical energy distribution between two particles was observed in 63 events, and an asymmetric distribution – in 9 events. The two groups of events were attributed to α-α and α-t quaternary fission, respectively (**Fig. 44a**). The events in which two α-particles were emitted at a very small angle to each other, were attributed to the pseudo-quaternary fission (decay of unstable short-lived ^{8}Be). Using the measured energies of alpha particles, the energy spectrum of emitted ^{8}Be particles was reconstructed (**Fig. 44b**). Also, the probabilities of true and pseudo-quaternary fission were determined, which are in agreement with the available experimental and theoretical estimates.

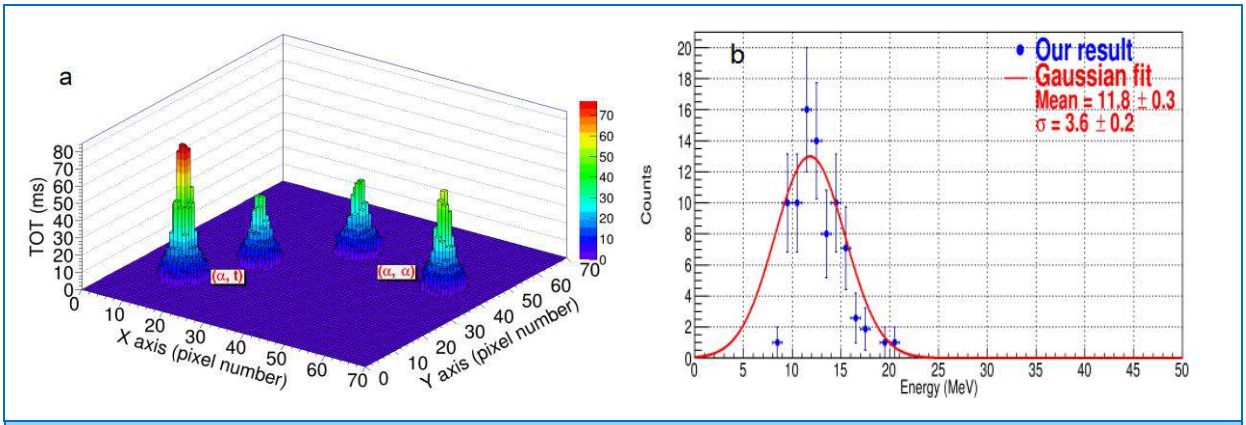

Fig. 44. (a) Examples of clusters for α-α and α-t coincidences; (b) Reconstructed energy spectrum for ^{8}Be.

Position-sensitive chamber for studying prompt fission neutrons

In connection with the development of a position-sensitive double ionization chamber a series of calculations was performed. The calculations of electrostatic fields and simulation of the detector response to fission fragments were made (**Fig. 45**). Formulas to calculate the coordinates of fission fragments in a three-dimensional Cartesian coordinate system were derived. The results of the numerical simulation of the detector have shown that due to the strip-like structure of the chamber anodes, it is possible to abandon the use of a Frisch grid. The DAQ system architecture was developed to acquire data from detectors using a 64-channel system of synchronization and digitization of detector pulses. It was demonstrated that the developed detector may be used for obtaining images of objects in neutron radiography at a pulsed neutron source.

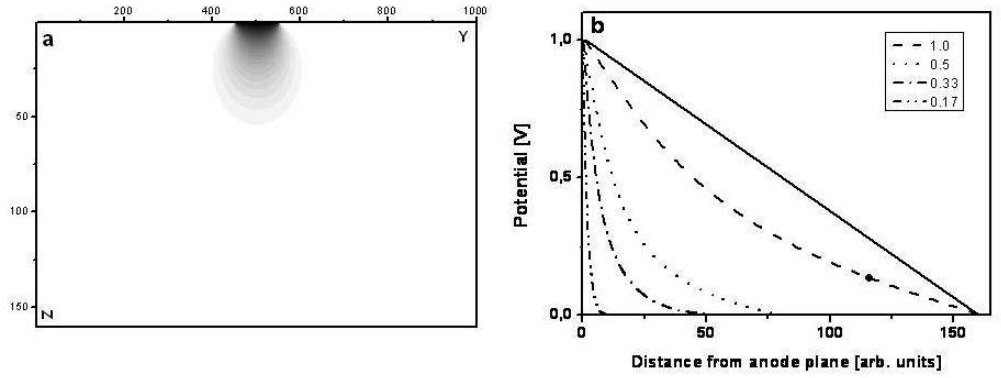

Fig. 45. Examples of calculations for weighting potentials forming signals from chamber electrodes

Investigations of (n,p), (n,α) reactions

The experimental and theoretical investigations of the (neutron, charged particle) reactions induced by fast neutrons were continued. The experiments are carried out at the Van de Graaf accelerators EG-5 in FLNP JINR and EG-4.5 of the Institute of Heavy Ion Physics of Peking University. Data on the neutron reactions with the emission of charged particles induced by fast neutrons are of much interest for studying the mechanisms of nuclear reactions and atomic nuclear structure as well as in choosing engineering materials and in performing calculations in the development of new facilities for nuclear power engineering.

The measurements of the ^{25}Mg(n,α)^{22}Ne and ^{54,56,nat}Fe(n,α) reactions were conducted. The data analysis for the measurements of the ^{57}Fe(n,α)^{54}Cr and ^{63}Cu(n,α)^{60}Co reactions at $E_n \sim 4.0$-6.5 MeV was completed; the results were published. The data treatment for the measurements of the ^{40}Ca(n,α)^{37}Ar reaction was completed; a paper was prepared for publication. For this nucleus the differential cross sections for ^{40}Ca(n,α_0), (n,$\alpha_{1,2}$), and (n,$\alpha_{3,4,5}$) reactions were measured at neutron energies of 4.0, 4.5, 5.0, 5.5, 6.0, and 6.5 MeV . The experimental values of the cross sections were compared with the calculations using the TALYS-1.6 code (**Fig. 46, 47**).

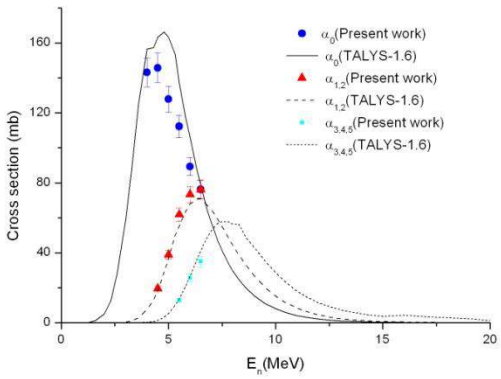

Fig. 46. The measured partial cross sections for the reactions ^{40}Ca (n,α_0), (n,$\alpha_{1,2}$) and (n,$\alpha_{3,4,5}$) compared with the calculations made by using the TALYS-1.6 code.

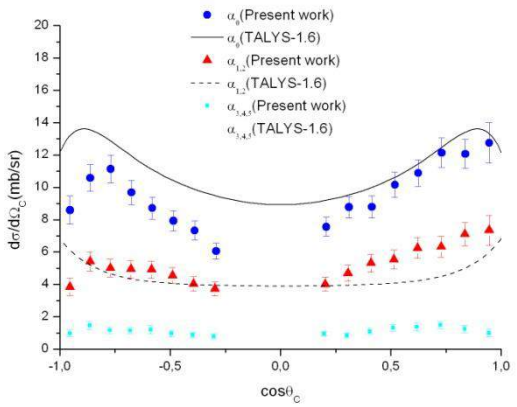

Fig. 47. Partial differential cross sections for the ^{40}Ca(n,α)^{37}Ar reaction in CMS at E_n = 5.5 MeV.

A systematic analysis of our experimental cross sections for the (n, α) reaction in the energy range from 4 to 6 MeV was performed. The dependence of these cross sections on the parameter (N-Z+0.5)/A in the specified energy range was observed and explained within the context of the statistical model.

Investigations of nuclear structure

A principally new variant of the practical model describing a cascade decay of an arbitrary level of a nucleus of any type with an excitation energy equal or greater than the nucleon binding energy, was proposed and fully tested. The complete absence of suitable for practical purposes theoretical models of the properties of excited levels with a structure determined by several quasiparticles and phonons called for the inclusion in this model of purely phenomenological concepts about the density of vibration-type levels and partial widths of their decay, in particular to define the shape of the energy dependence of the total density of quasiparticle and phonon levels at any nuclear excitation energies. The variation of these dependences for various functions of the excitation energy, as well as the analysis of approximated values of the parameters in the modified phenomenological representations showed that the change in the density of vibration-type levels (accurately reproducing the experimental values of the intensities of two-quantum cascades) is uniquely determined by the same parameter for nuclei with any weight and shape – the average nucleon coupling energy $\Delta = 12.8/\sqrt{A}$.

The number of broken Cooper pairs of nucleons below the coupling energy and their break-up thresholds is in agreement with the previously obtained values for the used variants of modification of the phenomenological part in the model. That is, the models that take into account the presence in the nucleus of the normal and superfluid phases and their interaction describe such parameters of the excited nucleus like the density of levels and the probability of their decay with radically better from the methodical viewpoint accuracy. Correspondingly, the statistical model of the nucleus (existing for more than fifty years), does not correspond to the present-day level in the experimental study of the nucleus.

The new experimental data on the intensities of two-quantum cascades in the nuclei of ^{52}V and ^{64}Cu obtained at the Dalat reactor (Vietnam) were analyzed in the framework of this model for gamma-decay of neutron resonances (**Fig. 48-50**). It was shown that these new data are fully reproduced by the model which takes into account the presence of a superfluid form of nuclear matter in an excited nucleus. These data do not fit to the existing representations of the nucleus as a purely fermionic system.

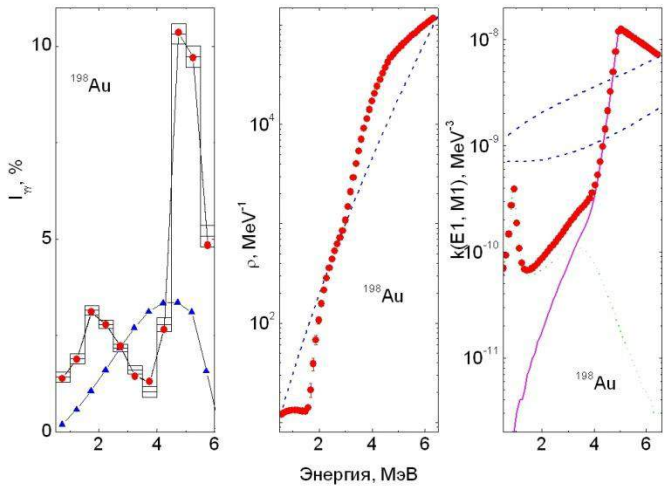

Fig. 48. Example of the resulting approximations of the modified model to the intensity of two-quantum cascades in the nucleus of ^{198}Au. Red points – approximation using the new model. Blue dots and lines – the result of calculation and model predictions of the most common functions of the level density (ρ) and radiation strength functions (k(E1) or k(M1)) of the statistical model of the nucleus.

1. SCIENTIFIC RESEARCH

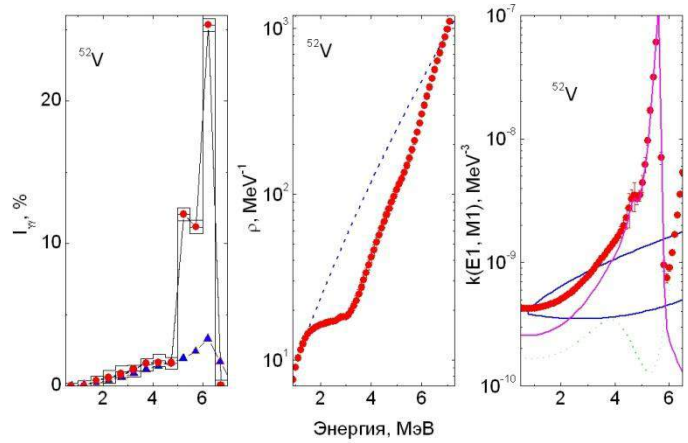

Fig. 49. Example of the resulting approximations of the modified model to the intensity of two-quantum cascades in the nucleus of ^{52}V. Red points – approximation using the new model. Blue dots and lines – the result of calculation and model predictions of the most common functions of the level density (ρ) and radiation strength functions (k(E1) or k(M1)) of the statistical model of the nucleus.

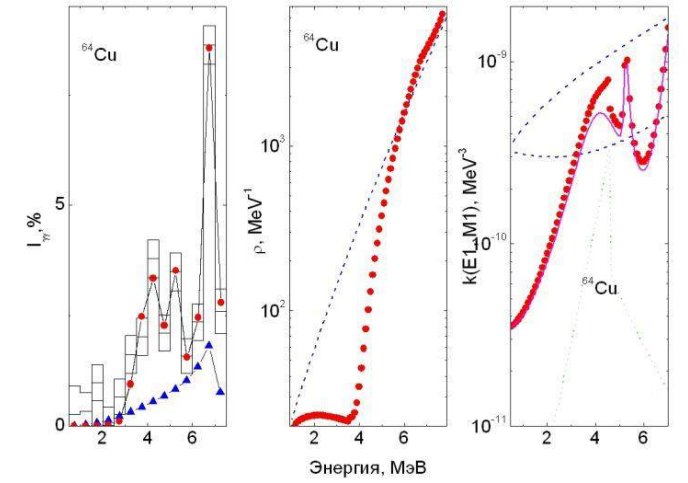

Fig. 50. Example of the resulting approximations of the modified model to the intensity of two-quantum cascades in the nucleus of ^{64}Cu. Red points – approximation using the new model. Blue dots and lines – the result of calculation and model predictions of the most common functions of the level density (ρ) and radiation strength functions (k(E1) or k(M1)) of the statistical model of the nucleus.

Design calculations of a helium UCN source at a thermal neutron beamline

At present, further progress in the physics of ultracold neutrons (UCNs) as a tool for nuclear physics research is often limited by the intensity of the available UCN sources. Therefore, in many world scientific centers projects of new advanced sources aimed at increasing the density and flux of UCN by 1-2 orders of magnitude are under development.

A helium UCN source was first proposed as early as in 1975 [6]. The principle of operation of such a source is based on the fact that neutron scattering in liquid helium ^{4}He can be accompanied by the generation of a phonon with an energy of 1.02 meV. If the neutron energy is slightly greater than 1.02 meV, the neutron is moderated down to ultracold energies. Thus, UCN can be generated from incident neutrons with energies within a very narrow range, since UCN energy is bounded from above by ~ 300 neV. The neutron could also generate two or more phonons in helium simultaneously. Both processes provide a comparable number of UCN for a wide range of incident cold neutron energies. It was also shown in the cited work that the produced UCNs could be stored in superfluid helium for a long time if the helium temperature is ~1 K or lower. This fact allows building up the UCN density in a source of this type up to very high values.

If we surround a UCN source containing liquid helium at temperatures below 1 K placed in a cold neutron beam by a cold neutron reflector producing UCN (i.e. make a trap for cold neutrons), this

makes it possible to significantly increase the cold neutron flux and, as a consequence, the UCN generation rate in the source. If as a reflector material we use a substance which is also a good thermal neutron moderator (and which is actually to be a source of cold neutrons), this allows us, first, to significantly increase the cold neutron flux and consequently the production capacity of the source, and, second, to use "cheap" thermal neutrons instead of "expensive" cold ones for producing UCN [6]. Thus, the maximum flux density in cold neutron beams at the reactor in ILL reaches ~ 10^{10} $cm^{-2}s^{-1}$, while the maximum flux density in a thermal neutron beam at the same reactor could be ~ 10^{11} $cm^{-2}s^{-1}$.

Such a UCN source surrounded by a moderator-reflector, which is a source of cold neutrons, is schematically shown in **Fig. 51**. The higher the albedo of the reflector, the higher the neutron flux density of the source (in the limit, when the albedo of the reflector is strictly equal to unity the neutron flux density accumulated in the cavity of the reflector is strictly equal to the flux density at the source — for the PIK and ILL reactors ~$10^{15}$$n \cdot cm^{-2}s^{-1}$).

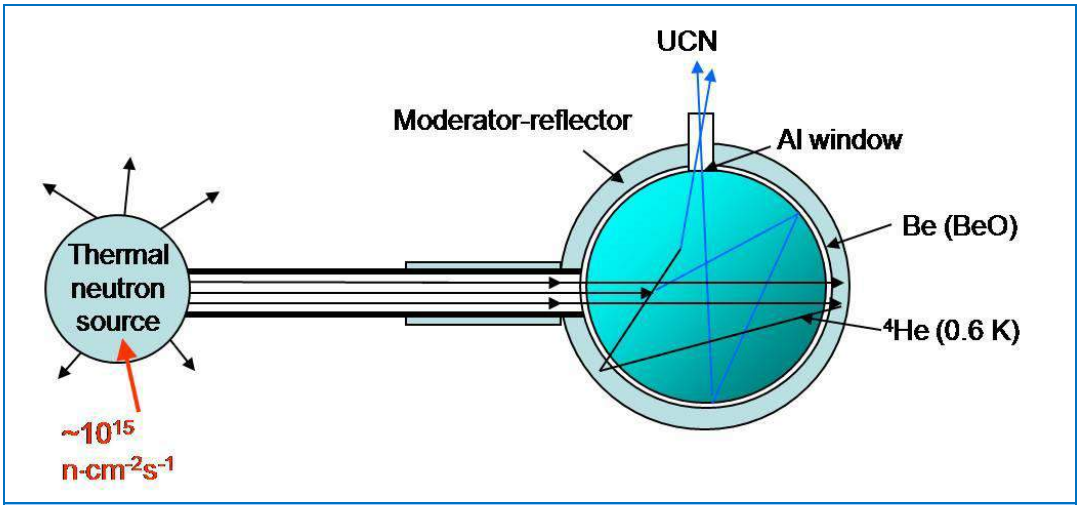

Fig. 51. Scheme of a UCN source surrounded by a moderator-reflector

A substance with the maximum albedo for cold neutrons, which we managed to find, is solid methane in phase II cooled to the temperature of ~ 4 K. Solid methane is, at the same time, one of the best cold moderators.

If a UCN source is positioned at the end of the neutron guide 20 cm in diameter directly behind the reactor biological shield, then the thermal neutron flux density at the entrance to the source is $1.2 \cdot 10^{11}$ $n/(cm^2 s)$ at the rector in ILL and $3.6 \cdot 10^{11}$ $n/(cm^2 s)$ at the PIK reactor. The respective integral fluxes are $3.8 \cdot 10^{13}$ n/s and $1.14 \cdot 10^{14}$ n/s.

To determine how the moderator-reflector made of solid methane operates, in 2013 the number and spectrum of neutrons accumulated inside the solid methane cavity were measured under the monochromatic neutron beam with a wavelength of 1.8 Å. In 2014 the computer simulation of the experiment was carried out using the program MCNP 4c with a special kern for solid methane. The results of the measurements and calculations are in full agreement (**Fig. 52**). This allowed us to calculate the parameters of the proposed UCN source. The results of these calculations are as follows: UCN volume density achieved in the source 40 cm in diameter installed at the reactor in ILL is $4.4 \cdot 10^4$ UCN/cm^3 at the UCN production rate of $5 \cdot 10^6$ UCN/s. The same source installed at the PIK reactor will give $1.3 \cdot 10^5$ UCN/cm^3 and $1.5 \cdot 10^7$ UCN/s, respectively. In this case, the UCN volume density in the source will be three orders of magnitude higher than that in the available UCN sources.

1. SCIENTIFIC RESEARCH

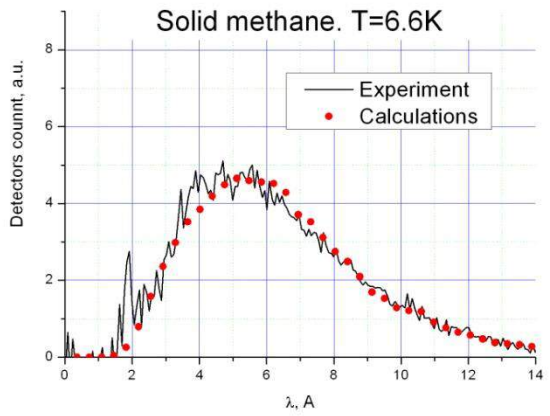

Fig. 52. Spectrum of neutrons accumulated in the methane cavity. Thin black line – results of the measurements. Points – results of numerical simulation of the experiment.

Cooperation in the framework of the GRANIT project in ILL (France)

FLNP JINR in cooperation with the P.N.Lebedev Physical Institute of RAS and Virginia State University (USA) are the members of the GRANIT collaboration. The GRANIT project aimed at designing and building a second-generation gravitational neutron spectrometer with ultra-high energy resolution GRANIT (**GRA**vitational **N**eutron **I**nduced **T**ransitions).

In 2014, in the framework of the development of the spectrometer the loss factor in the sapphire neutron guide (under construction) was measured. The measured probability of losses in the neutron guide was $3 \cdot 10^{-4}$ per reflection event. The spectral independence of the losses points to the absence of neutron gaps in the neutron guide. Upon outgassing or cooling down to liquid-nitrogen temperatures the probability of losses drops several times. This will allow one to apply a new neutron guide system with significantly improved characteristics in the coming year.

Continuation of the experiment to test the weak equivalence principle for the neutron

The experiment to verify the weak equivalence principle for the neutron was continued with the Epigraph gravitational spectrometer built in 2010 and significantly improved in 2011. The operation of the instrument is based on the combined use of Fabry-Perot neutron interferometers and a neutron flux modulator-chopper. The change in the energy of the neutron mgH falling in the gravitational field is compared with the energy transferred to the neutron diffracted into the –1 order by a moving diffraction grating.

A specific feature of the instrument is the possibility of using an original time-of-flight technique based on a periodic modulation of the neutron flux and on measurements of the oscillation phase of the detector count rate. The UCN detection is synchronized with the modulator. A high degree of beam monochromatization ($\Delta v/v < 2\%$) makes it possible to work with the times of flight, which manifold exceed the modulation period, thus ensuring a unique energy resolution of the instrument.

In 2014:

1. The results obtained in the previous measurement cycle were analyzed.
2. Possible reasons for several systematic effects revealed earlier were analyzed.
3. A new software package to control the elements of the instrument, data acquisition and primary processing was designed. Using this package the frequency of the modulator-chopper and the rotating grating can be tuned and stabilized, as well as the analyzing filter can be moved along the vertical direction. For data acquisition and primary processing a stand-alone module E 20-10 with a four-channel ADC (sampling frequency of 10 MHz, data buffering) is used. Data interchange with a PC is via a USB port. Due to specific features of the PF2 UCN

source, with which the experiments are carried out, the operation of the program is synchronized with the device distributing beams from the UCN source.

4. To better understand the operating peculiarities of the instrument and to identify systematic errors, the MC simulation of the spectrometer using the Geant4-UCN software package was started.

In the measurement cycle (started on November 3) on the UCN beam in ILL (Grenoble) at least three origins of systematic errors, which occurred in the measurements in 2012, were found.

TOF Fourier spectrometry of UCN and experimental investigation of UCN spectra at diffraction from a moving grating

When analyzing the results of the experimental data obtained in 2012, it was realized that the used phenomenon of quantization of neutron energy at diffraction from a moving grating is not well studied both theoretically and experimentally. In 2014 we made significant efforts to fill this gap. The experimental study of this phenomenon included the following activities:

1. The experimental data of test experiments in Fourier spectroscopy of ultracold neutrons were analyzed.
2. The Monte Carlo simulations of TOF Fourier spectra and their analysis were performed.
3. A new modulator of the spectrometer (**Fig. 53**) with a corresponding stator was designed and manufactured.

In the measurement cycle (started on November 3) on the UCN beam in ILL (Grenoble) the TOF Fourier spectrometry technique was successfully tested and TOF UCN spectra measured with three different types of interference filters were obtained.

A multiwave dynamic theory of neutron diffraction from a moving phase grating was developed in the framework of the approximation of slowly varying amplitudes in cooperation with V.A.Bushuyev (Moscow State University). The effect of the speed of the grating, its period and the height of grooves on a discrete energy spectrum and intensities of diffraction peaks of various orders was analyzed. As an extension of the previous studies by A.I.Frank, in which the possibility of a negative time delay in the neutron reflection from multilayer structures was predicted, the analysis of the concept of a group time delay (GTD) in the reflection of electromagnetic waves and neutrons from resonant and nonresonant media and layered structures was carried out in cooperation with V.A.Bushuyev.

Fig. 53. Multi-slit Fourier-chopper of the Epigraph spectrometer.

The relationship of GTD with a pulse time delay and spatial longitudinal beam shifts was considered. The arising pseudoparadoxes, as well as the effect of GTD on the shape of reflected pulses and beams were discussed. The calculations of quantum effects in neutron transmission through a high-frequency quartz oscillator were started. Within the context of the effective potential model this object is represented as an area of the potential with boundary and magnitude, which are

periodically dependent on time. The difficulty of these quantum calculations stems from the fact that the neutron propagation time through a medium (10^{-4} s) is much larger than the oscillation period (5×10^{-7} s) (**Fig. 54**).

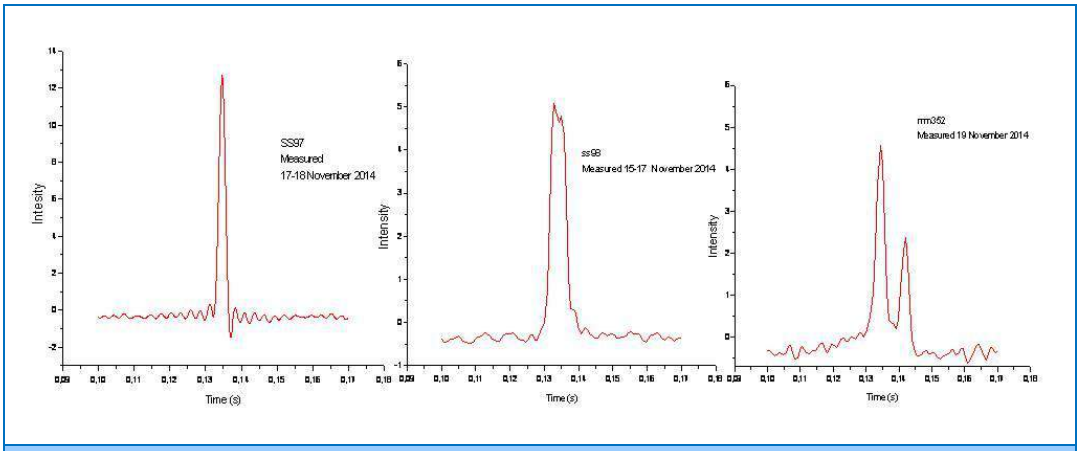

Fig. 54. Time-of-flight spectra obtained with interference filters using Fourier spectroscopy. From left to right: five-layer filter with a narrow bandwidth of about 4 neV, nine-layer filter with a wide bandwidth of about 10 neV and five-layer filter with connected resonators and a splitted band.

II. Methodological and applied research

Analytical and methodological investigations at the IREN facility

On the IREN facility the effect of neutron and gamma radiation on plastic scintillators used in the CMS experiment at CERN was investigated. Three years of operation experience with the hadron calorimeter have shown an unexpectedly large reduction in light output of plastic detectors. It was concluded that not all the factors of the radiation influence on the scintillators were taken into account. To clarify this issue, plastic scintillators of four types, namely SCSN-81, UPS-923A (manufactured in Kharkov), BC-408, LHE (manufactured in Dubna) were studied. The irradiation was carried out on the IREN resonance neutron source with the maximum exposure time of up to 30 days. The light output of the samples with different shapes before and after irradiation was compared. No significant effect of the irradiation rate on the light output was revealed. There is a large amount of bronze between the scintillators in the CMS experiment, therefore the influence of the additional induced radioactivity emitted by radioisotopes that emerged as a result of neutron irradiation of bronze was studied. For this purpose, two identical scintillators SCSN-81 were irradiated at the same distances from the target of IREN, but behind one of the scintillators a bronze disc had been placed. The measurements of light output have shown that there is a significant contribution of the induced radioactivity. The results of the measurements are confirmed by the calculations using the FLUKA program.

In 2014, the measurements and data treatment related to the search for cosmic dust in the samples provided by the Sternberg Astronomical Institute, MSU, were completed. The measurements were performed on the IREN facility. The samples from expeditions of 2010 – 2011 in the region near the Aktru glacier (North Chui Ridge of Altai) were analyzed (**Fig. 55**).

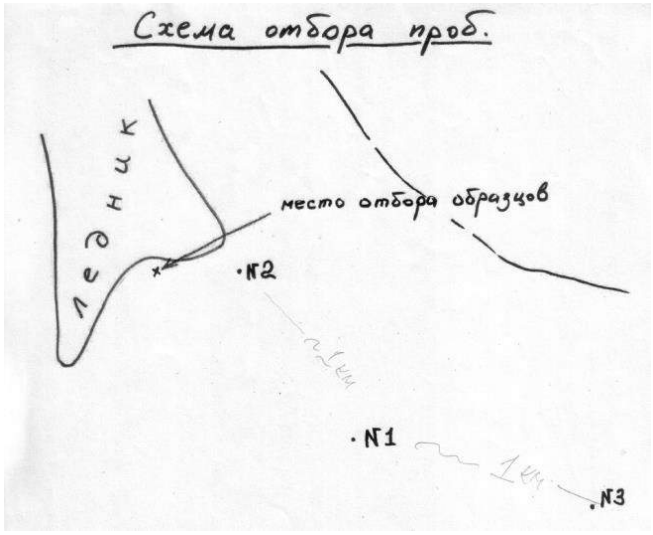

Fig. 55. Sample collection place near the glacier.

The point X denotes the place where the samples of bottom sediments accumulated in the rock cavities of the stream bed were collected. At points 1-3 control soil samples of glacial moraines were collected from several horizons: surface, at a depth of 0.3 m; 0.6 m. The distance between points 1-3 is about 1 km. The analysis was performed using the neutron spectroscopy technique. The results of the study are given in **Table 1.**

Table 1. Results of sample analysis.

Sample collection place	Depth, m	Sample weight, g	Mass of iron in sample, g	Weight fraction of iron in sample, %
Point X		270	12.6 ± 2.4	4.7± 0.9
Point №1	0.0	470	10.98±1.77	2.34±0.37
	0.3		14.05±1.6	3.0±0.34
	0.6		8.59±1.9	1.83±0.40
Point №2	0.0		14.02±4.0	3±0.9
	0.3		13.4±2.1	2.8±0.4
	0.6		11.15±2.56	2.4±0.5
Point №3	0.0		9.30±1.30	1.98±0.30
	0.3		15.8±2.37	3.36±0.5
	0.6		17.21±1.38	3.66±0.29

Analytical investigations on charged particle beams of the EG-5 accelerator

In 2014 the EG-5 accelerator was in operation for various experiments for about 495 hours. The main research area is the elemental analysis of surface layers of solids using nuclear analytical techniques: RBS (*Rutherford Backscattering Spectrometry*) and ERD (*Elastic Recoil Detection*). The experiments were conducted in cooperation with a number of Russian and foreign research institutes:

A.M.Prokhorov General Physics Institute of RAS (Moscow), B.P.Konstantinov Petersburg Nuclear Physics Institute (Gatchina), Voronezh State University, Marie Curie-Sklodowska University (Lublin, Poland), Institute of Electrical Engineering of the Slovak Academy of Sciences (Bratislava, Slovak Republic), Institute of Applied Physics of the National Academy of Sciences of Ukraine, VINCA Institute of Nuclear Sciences, University of Belgrade, Serbia. In addition, the specialists from DLNP carried out experiments to investigate the characteristics of matrix gallium-arsenide semiconductor detectors on charged particle beams of the EG-5 accelerator.

Analytical investigations at the IBR-2 reactor

Development of the NAA Sector experimental base

In the reporting period in the NAA&AR Sector a software package for complex automation of multielement neutron activation analysis (NAA) at the IBR-2 reactor [7] was developed and three automatic sample changers (SC) were installed to automate mass measurements of spectra of irradiated samples on three detectors. A new switch cabinet for spectrometric electronics and controllers to control the SC provided their operation at a specified temperature. After the completion of the installation work the final tuning of the program for the automation of spectrum measurements using the NAA database was made. The activities on automation of NAA are conducted in the framework of the IAEA Coordinated Research Project «Development of an Integrated Approach to Routine Automation of Neutron Activation Analysis" (F1.20.25/CRP1888, Contract No. 17363).

During the reactor maintenance shutdown in the summer the adjustment of operation of the pneumatic transport system with a new compressor as well as the installation of an air conditioner and suction-and-exhaust ventilation system in room 129a of the REGATA facility were carried out.

For the purpose of carrying out elemental analysis by atomic absorption spectrometry (AAS) a Thermo Scientific *iCE 3500 Atomic Absorption Spectrometer*, suction-and-exhaust ventilation system and an exhaust fume hood were installed in accordance with the requirements for laboratories working with acids used in the analysis of samples by AAS. Upon the completion of the installation work the specialists from Intertech Corporation carried out the start-up and adjustment of the atomic absorption spectrometer and issued a certificate of release to service. In the same building a low-background HPGe detector with shielding was installed for conducting planned radioecological studies.

Methodological work

In connection with the beginning of joint work with the *Astrobiology Sector* of the N.M.Sissakian *Laboratory* of Radiation Biology, JINR, on the determination of the elemental composition of meteorites, as well as to assess the capabilities of automatic sample changers on the detectors the methodological studies were performed to determine the concentrations of elements for some medium- and long-lived isotopes of meteorites by means of measuring induced gamma activity spectra within a few hours after short-term irradiation. Samples were irradiated for 1-3 min with subsequent acquisition of spectra immediately after irradiation, and then with a delay ranging from a few hours up to tens of hours.

The libraries of short-lived isotopes used for standard mass measurements of element concentrations were corrected and supplemented with data for a number of medium- and long-lived isotopes. Thus, for isotopes with a half-life of several tens of hours and even years a technique was developed for determining the element concentration in some specific samples after short-term exposures. The need for using single-element standard samples with specified parameters (and consequently the necessity of their purchase) was identified.

Biomonitoring of air pollution

In 2014, in the framework of the international program "Heavy metal atmospheric deposition in Europe – estimations based on moss analysis" the work to study the environmental situation in the ferrochrome production area in the Tikhvin District of the Leningrad Region was completed [8]. The obtained results were included in the Annual Report of the UN Commission on the long-range transport of air pollutants in Europe. In the framework of the RFBR grant (№ 14-05-31279) for young scientists “My first grant”, 170 moss and soil samples were collected on the territory of Moscow and Tver regions. A multivariate statistical analysis of NAA data was performed, and distribution maps of pollutants on the territory under study were plotted using the GIS technology.

A long-term cooperation with the Slovak specialists in biomonitoring of atmospheric depositions of trace elements found its reflection in chapter "Atmospheric pollution”. The study of atmospheric depositions of heavy metals and radionuclides around the Temelin nuclear power plant in Czech Republic was completed [9]. During the reporting period two studies were made on data analysis of atmospheric depositions of heavy metals and other elements in Albania. In the framework of the Serbia-JINR Collaboration Program a comparative analysis of air pollution in the so-called "street canyons" of Moscow and Belgrade was performed. The neutron activation analysis of moss samples collected by teachers and students in the national parks of Poland was done in the framework of the Program of Poland-JINR collaboration.

The study on the determination of element concentrations in moss-biomonitors collected in the area around the Kardzhali lead-zinc plant – one of the most ecologically adverse places in Bulgaria was completed. The obtained results were used in the bachelor's thesis work of a Bulgarian student in 2014. In the near future the NAA of soil samples from the same environmental "hot spots" of Bulgaria will be completed.

Biotechnologies

In 2014, in collaboration with the E.Andronikashvili Institute of Physics, I.Javakhishvili Tbilisi State University and I.Chavchavadze State University *(*Tbilisi*,* Georgia) the studies were continued on the development of methods for synthesis of silver and gold nanoparticles by new species of microorganisms – Archaea. The strain of thermo-acidophilic crenarchaeon *Sulfolobus islandicus* LAL14/1 provided by the Pasteur Institute (Paris, France) was used to obtain silver and gold nanoparticles at high temperatures (75 C). In combination with a number of optical and analytical methods the neutron activation analysis at the IBR-2 reactor was used to characterize the processes of synthesis of gold and silver nanoparticles by the Archaea strain, whose application for technological purposes has been very limited so far [10].

In 2014, the joint investigation carried out in cooperation with the Institute of Microbiology and Biotechnology of ASM was continued to study the process of removing toxic metals (chromium, nickel) from wastewater using microalgae *Spirulina platensis*. Also, studies were conducted to monitor changes in the content of the main components of *Spirulina* biomass (proteins, carbohydrates, and others) in the process of formation of silver nanoparticles by microalgae [11].

In the framework of a pilot project in cooperation with the University of Oulu, Finland the potential of NAA for analysis of pine sawdust used in wastewater treatment as a sorbent of metals was demonstrated. In cooperation with the Institute of Environmental Engineering of Óbuda University (Budapest, Hungary) similar investigations were conducted in a model experiment on the use of *Miscanthus sinensis* plant as a sorbent of metals. The study is a part of a PhD thesis of a Hungarian postgraduate student of Óbuda University.

In collaboration with the Institute of Water Problems of RAS the elemental composition of cyanobacterial communities (extremophiles) living in hot springs of Kamchatka at temperatures above 55 C was determined using epithermal NAA.

1. SCIENTIFIC RESEARCH

Environmental assessment

In 2014, the multielement analysis of soils and bottom sediments from various regions of the Nile delta and its near-shore area was continued in the framework of the joint JINR-Egypt project «Assessment of the environmental situation in the delta of the Nile River using nuclear and related analytical techniques». The obtained results have shown that the element composition of these samples is determined mainly by geochemical features of the region under study and is not affected by the anthropogenic load.

Within the framework of the Cooperation Agreement with the Institute of Biology of the Southern Seas (Sevastopol) to assess the state of the coastal ecosystem of the Crimea, the analysis of macroalgae-biomonitor samples in the coastal zone of the Black Sea was completed. The cleanest water areas of the coastal zone of the Crimea were found and for the algae the background concentrations of about 30 macro- and microelements were determined [12]. A technique of sampling and preparation of phytoplankton for NAA on the IBR-2 reactor was optimized and the element composition of 50 samples was determined. The concentrations of 46 elements in the phytoplankton of the Black Sea were obtained for the first time. The effect of the elemental composition on the biophysical parameters of the functional activity of phytoplankton communities in coastal areas was assessed. The obtained results have shown that phytoplankton can be successfully used as a biomonitor of water ecosystems [13].

In cooperation with Moscow State University (Faculty of Biology) the investigation on the determination of the elemental composition of soil, bottom sediments, terrestrial and aquatic vegetation was started to assess the transport of pollutants in the strategically important areas of the Black Sea (coastal zone of Anapa, Novorossiysk and Tuapse) .

In collaboration with the University in Stellenbosch, South Africa, complex investigations of air pollution using mosses and lichens as well as of water ecosystem (Saldanha and Danger bays) in the Atlantic Ocean, West Coast of South Africa, were continued in the framework of the project "Mollusks as Biomonitors of Water Ecosystems in the Republic of South Africa".

Analysis of food products

The studies were completed and a joint paper (in cooperation with the analytical center of the Geological Institute of RAS) on the application of nuclear-physical analytical methods for studying the quality of foodstuffs, in particular, for the determination of Cl, Br, I and Se in the human organism.

The NAA was used to study the elemental composition of some agricultural crops (cereal crops and vegetables) grown using bioenergoactivator "Biorag" developed by biochemists of I.Javakhishvili Tbilisi State University, as well as to analyze the respective soil samples. The soil composition shows good agreement with the mean values characteristic for terrestrial rocks. The results of NAA for the investigated samples revealed no toxic elements in the agricultural crops grown using the bioenergoactivator. Moreover, the content of heavy metals in all cases decreased, which is indicative of a positive effect of the innovative product on the elemental composition of the agricultural crops [14].

The results of NAA of edible oils (sunflower and olive oils) from Romania have revealed a significant difference in their elemental composition, which is in agreement with the published data obtained by other methods. The concentrations of heavy metals do not exceed the guideline values recommended by the World Health Organization for food products [15].

Geology

In 2014, in the framework of the joint JINR-Romania project with University of Bucharest the investigation of geochemistry of the Black Sea was continued. Using NAA the elemental composition of the vertical profiles of bottom sediments was studied. The study of geochemistry of loess samples

of the Quaternary Period collected in the Dobruja region (Romania) made it possible to obtain information about the climate of the Quaternary Period.

In cooperation with the Western Cape University (South Africa) the NAA study of coal fly ash from the Matla coal power station in the Mpumalanga province in South Africa was conducted. The analytical advantages of NAA using epithermal neutrons in determining the elemental composition of ash were demonstrated over such methods as inductively coupled plasma atomic emission spectroscopy (ICP-AES), laser ablation inductively coupled plasma mass spectrometry (LA ICP-MS) and X-ray fluorescence (XRF).

Analysis of materials of extraterrestrial origin

In 2014, the study aimed at searching for cosmic dust in peat columns collected in Siberia and in the meltwater from the high-mountain glacier Aktru in Altai was completed. The age determination of peat column layers was carried out at the Adam Mickiewicz University in Poland. The particles detected by means of electron microscopy along with the results of the neutron activation analysis of peat column samples (judging from the iron/nickel concentration ratio) allow us to assume that these particles could be of extraterrestrial origin. The identification of the material collected using magnetic traps in the meltwater from the glacier in Altai is more controversial.

Studies of a peat column from the site of the Tunguska meteorite fall in 1908 have started in cooperation with the specialists from the Adam Mickiewicz University (Poland) who have extensive experience in dating (age determination) of samples and interpretation of data of the retrospective element analysis of peat columns.

Anthropological research

In the framework of the RFBR project (№12-06-00096/14 due to be completed in 2014) in cooperation with the Moscow State University (D.N.Anuchin Research Institute and Museum of Anthropology*)* the NAA of hair samples of a representative group of children from the Ongudaysk District of the Altai Republic as well as soil and plant samples from the places of their residence was continued to find possible correlations between their elemental composition and to reveal the endemic features of the effect of the geochemical environment on the human body.

Medicinal plants

The analysis of medicinal plants using NAA has become a new promising line of research in the NAA&AR Sector. These investigations are carried out in cooperation with specialists from Mongolia, Poland and Bulgaria. The study on the analysis of traditional Mongolian plants (*Carduus crispus L., Sanguisorba officinalis, Granium pratense, Chamaenerion angustifolium (L)Scop*) used in herbal medicine won Thomas Edison Award-2014 (PHOTON Foundation «…The authors receive Thomas Edison Award-2014 in the domain of Medicinal Plants for Inspiration and Knowledge Distribution among young research scholars») [16].

https://sites.google.com/site/photonfoundationorganization/home/international-journal-of-medicinal-plants.

Materials science

In 2014, in the framework of the BRFBR-JINR joint grant and in cooperation with the Scientific and Practical Materials Research Center of the National Academy of Sciences of Belarus, the investigations of the crystallization processes and the characterization of artificial diamonds in the C-Mn-Ni-Fe system were conducted. In the course of the experiment diamond crystals were obtained in the Fe-Ni-C and Mn-Ni-C systems at a pressure of 5 GPa and a temperature of 1700 K. The use of NAA allowed us to study the impurity composition of the diamonds. The electronic microscopy study was performed using a scanning electron microscope Hitachi SU8000 in the N.D.Zelinsky Institute of

1. SCIENTIFIC RESEARCH

Organic Chemistry (Moscow) under the grant for short-term scientific and educational training in the field of electron microscopy. Electron microscopy was used to determine the size and shape of the obtained crystals. It has been found that despite the similarity in the crystal formation mechanism, their characteristics differ significantly. In the Fe-Ni-C system crystals have a more perfect geometry and larger sizes. From the impurity composition data it follows that in the Mn-Ni-C system the process of nucleation is stimulated resulting in the formation of smaller crystals with lesser hardness and imperfect shape. Thus, by using a specific catalyst system, it is possible to obtain crystals with specified characteristics. Also, a joint project was started aimed at studying phase formation processes and physical characteristics of the compounds in the Cu-Fe-S system at high pressures and temperatures. A part of the experimental material was sent to the University of Galaţi, Romania, to perform X-ray diffraction and scanning electron microscopy analyses.

References

1 Исследования в области нейтронной ядерной физики http://wwwinfo.jinr.ru/plan/ptp-2014/r441104.htm.

2 Development of the tagged neutron method for elemental analysis and nuclear reaction studies (project TANGRA), http://indico.jinr.ru/materialDisplay.py?contribId=7&materialId=0&confId=759.

3 Enik T.L., Likhachev A.N., Mitsyna L.V., Popov A.B., Salamatin I.V., Sirotin A.P., AURA setup testing at IREN neutron beam. JINR Preprint E3-2014-13, Dubna, 2014.

4 Enik T.L., Mitsyna L.V., Popov A.B., Salamatin I.M., The Angular Anisotropy of Slow Neutrons Scattering Measured at IREN Facility with Vanadium as a Sample. JINR Preprint E3-2014-27, p. 42.

5 Golub R., Pendlebury J.M., Super-thermal sources of ultra-cold neutrons. (1975) Physic Letters A, v. 53, p. 133-135.

6 Baessler S. et al., New methodical developments for GRANIT. (2011) Comptes Rendus Physique, v. 12, p. 729.

7 Pavlov S.S., Dmitriev, A.Yu. Chepurchenko I.A., Frontasyeva M.V., (2014) Automation system for measurement of gamma-ray spectra of induced activity for neutron activation analysis at the reactor IBRr-2 of Frank Laboratory of Neutron Phsyics at the Joint Institute for Nuclear Research. Physics of Elementary Particles and Niclei, v. 11, p. 737–742.

8 Vergel K.N., Goryainova Z.I., Vikhrova I.V., Frontasyeva M.V., (2014) Moss biomonitoring and employment of the GIS technology within the framework of the assessment of air aollution by industrial enterprises in the Tikhvin District of the Leningrad Region. Ecology of Urban Areas, v. 2, p. 92-101.

9 Thinova L., Frontasyeva M., Vergel K., Bayushkina E., (2014) Assessment of contamination with trace elements and man-made radionuclides around Temelin Nuclear Power Plant in Czech Republic. Radiation Physics and Chemistry, v. 104, p. 432-435.

10 Kalabegishvili T. L., Murusidze I. G., Prangishvili D. A., Kvachadze L. I., Kirkesali E. I., Rcheulishvili A. N., Ginturi E. N., Janjalia M. B., Tsertsvadze G. I., Gabunia V. M., Frontasyeva M.V., Zinicovscaia I., Pavlov S. S., (2014) Gold nanoparticles in sulfolobus islandicus biomass for technological applications. Advanced Science, Engineering and Medicine, v. 6, p. 1302-1308.

11 Zinicovscaia I., Cepoi L., Rudi L., Chiriac T., Valuta A., Duca Gh., Kirkesali E., Frontasyeva M.V., Culicov O., Pavlov S.S., Bobrikov I., (2014) Biochemical changes in some cultures of

cyanobacteria at the synthesis of silver nanoparticles. Canadian Journal of Microbiology, doi: 10.1139/cjm-2014-0450

12 Kravtsova A., Milchakova N., Frontasyeva M., (2014) Accumulation of macro- and trace elements in brown algae Cystoseira studied by multielement instrumental neutron activation analysis (the Black Sea, south-western Crimea). Ecological Chemistry and Engineering, v. 21, p. 9-23.

13 Nekhoroshkov P.S., Kravtsova A.V., Frontasyeva M.V., Tokarev Yu. N., (2014) Neutron activation analysis and scanning electron microscopy of phytoplankton in the coastal zone of Crimea (The Black Sea). American Journal of Analytical Chemistry, v. 5, p. 323-334.

14 Frontasyeva M.V., Pavlov S.S., Zinicovscaia I.I., Bagdavadze N. V., Kirkesali E.I., Gakhokidze R., (2014) Neutron activation analysis of agricultural crops exposed to bioenergoactivator. Agricultural Chemistry, v. 6, p. 55-61.

15 Culicov O. A., Zinicovscaia I., Setnescu T., Setnescu R., Frontasyeva M. V., (2014) Elemental content of edible oils studied by neutron activation analysis. Accepted by Revue Roumaine de Chimie, 2014.

16 Baljinnyam N., Tsevegsuren N., Jugder B., Frontasyeva M.V., Pavlov S.S., (2014) Investigation of elemental content of some Mongolian medicinal plants. International Journal of Medicinal Plants. Photon, v. 106, p. 481-492.